

Achieving High Stiffness Range of Force Feedback Gloves using Variable Stiffness Mechanism*

Yuan Guo, Dangxiao Wang, *Senior Member, IEEE*, Ziqi Wang, Xiuping Yang, Haitong Wang, Yuru Zhang, *Senior Member, IEEE*, Weiliang Xu, *Senior Member, IEEE*

Abstract— Force feedback glove is a promising interface for producing immersive haptic sensation in virtual reality and teleoperation systems. One open problem of existing gloves is to simulate virtual objects with adjustable stiffness in a fast dynamic response, along with lightweight and good back-drivability. In this paper, we introduce a leverage pivot modulating mechanism to achieve variable stiffness simulation for force feedback gloves. To simulate free space operation, the revolute pairs of the mechanism move in the unlocked state, which allows the user to clench his/her fist or fully extend fingers. To simulate constrained space operation, the revolute pairs are locked and passive feedback forces are generated at the fingertip. The total weight of the single-finger prototype glove is 55g. Experimental results show that the backdrive force of the glove is less than 0.069N in the free space, and the fingertip force reaches up to 12.76N in the constrained space. The stiffness of the glove is tuned by changing its structural stiffness, which ranges from 136.96Nmm/rad to 3368.99Nmm/rad.

I. INTRODUCTION

Force feedback glove transforms the way that people interact with virtual environment, which changes haptic interfaces from the handle-hold interactive mode of desktop devices (such as Phantom desktop) to the free-grasping interactive mode of wearable devices with multi-finger coordination. By exploiting the dexterous manipulation and sensitive perception capabilities of our hands, force feedback gloves allow users to touch and manipulate virtual objects in an intuitive and direct way, and enhance greatly interactive immersion.

In the past three decades, a large number of force feedback gloves has been developed [1, 2]. According to actuation principles, existing force feedback gloves can be generally classified into three categories: pneumatic and/or hydraulic actuators [3], electric motors [4] and actuators using functional materials [5].

*Research supported by the National Key Research and Development Program under Grant No. 2017YFB1002803, and by the National Natural Science Foundation of China under the grant No. 61572055, and No. 61631010.

Y. Guo, D. Wang, Z. Wang, X. Yang, H. Wang and Y. Zhang are with the State Key Lab of Virtual Reality Technology and Systems and Beijing Advanced Innovation Center for Biomedical Engineering, Beihang University, No. 37 Xueyuan Road, Haidian District, Beijing, China. 100191. (TEL: + 86-10-82338273; Email: hapticwang@buaa.edu.cn).

D. Wang is also with Peng Cheng Laboratory, Shenzhen, Guangdong Province, 518055, China.

W. Xu is with Department of Mechanical Engineering, University of Auckland, Auckland 1142, New Zealand. He is also with Beijing Advanced Innovation Center for Biomedical Engineering, Beihang University, Beijing, China.

The pneumatic/hydraulic force feedback gloves have the advantages of lightweight and wide motion range. But due to the time delay of pumps and valves, these gloves are difficult to provide haptic feedback with kHz update rates and the response time is greater than 100ms. Moreover, complicated and bulky power transmission systems, such as pneumatic/hydraulic pump and pressure reducing valve, limit the portability of devices.

Force feedback gloves driven by functional materials are promising, but there are still many open problems to be solved. For example, shape memory alloy [6] has low response frequency and poor control precision; dielectric elastomer material [7] is driven by high voltage and needs to ensure electrical safety; artificial muscle [8] is difficult to manufacture and production cost is high; the back-drivability of magnetorheological fluid [9] is poor and its excitation device is bulky. It seems a long way to see the breakthrough of novel function materials to produce high performance gloves.

Compared with the above two types of actuation principles, force feedback gloves driven by electric motors have the characteristics of fast response, high control precision and portability. Classical force feedback gloves driven by electric motor, such as CyberGrasp [10], realize the force feedback through the way that motor drives the cable. RML glove [11] achieves the force feedback by the combination of motors, cables and links. These gloves can provide active force and simulate virtual objects with different stiffness. However, the disadvantage is that the transmission system becomes complex, and the power consumption of devices is increased with the simulated stiffness of virtual object.

In order to make lightweight haptic gloves, recently, passive force feedback concepts have been introduced, which aim to reduce the structural complexity and weight of gloves. Dexmo [12] realizes passive feedback forces by driving two stopping sliders and locking the ratchet wheel firmly in place, which can provide binary haptic feedback. The Wolverine [13] system provides a large range of motion and high passive resistance forces reaching 106N through the ingenious mechanisms. The above passive solutions effectively reduce the weight and is inherently safe, but lose the ability to simulate objects with variable stiffness.

Inspired by the pros and cons of electric-driven passive force feedback concepts [12, 13], in this paper, we propose a mechanism that can enable adjustable stiffness simulation for passive force feedback gloves. The contributions of the proposed study can be summarized in the following:

(1) In order to simulate variable stiffness while reducing the power consumption, we introduce a mechanism that can directly changes its structural stiffness. The proposed variable stiffness mechanism realizes the stiffness regulation by changing the position of pivot through a rack-pinion transmission mechanism. It has the advantages of fast response speed and high control accuracy, and can provide different stiffness information according to the softness of virtual object. The theoretical adjustable range of the stiffness is from zero to infinity, but due to the limitation of material and structural layout, the maximal and minimal stiffness is 3368.99Nmm/rad and 136.96Nmm/rad respectively.

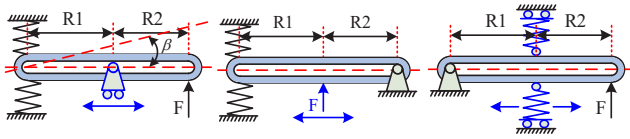
(2) A single-finger force feedback glove with variable stiffness was developed. Experimental results show that the proposed glove could allow full hand open/closing and provide variable feedback force. The maximum resistance force is 0.069N in simulating free space. While simulating constrained space, the feedback force reaches up to 12.76N in the fingertip. In addition, the total weight of the single finger prototype is 55g.

II. VARIABLE STIFFNESS MECHANISM

A. Principle of Variable Stiffness

Different from the constant stiffness mechanism, the variable stiffness devices usually use elastic components to realize the stiffness variation. According to mechanical structure, variable stiffness mechanism can generally be classified into five categories [14]: triangle structure [15], four-bar structure [16], lever structure [17], special surface structure [18], S-shaped rotating structure [19]. Based on the consideration of adjustable range of stiffness, spatial layout of device and motion range, the type of lever structure is selected in this paper.

There are three key factors for the design of variable stiffness mechanism with the lever structure, which are the acting point of external force, the connection position of the spring and the pivoting position of the lever [20]. By changing the combination method of these three factors, the variable stiffness mechanism can be divided into three sub-types as shown in Fig. 1. Where F denotes the external force, R_1 and R_2 denote the distance between the acting point of external force, the connection position of the spring and the pivoting position of the lever.



a) Movable pivot b) Movable force-acting point c) Movable spring position
Figure 1. Sub-types of variable stiffness mechanisms with a lever structure (adapted from [14, 20])

For the sub-type lever mechanism with movable force-acting point, the effective arm length of the lever mechanism is R_2 . The shorter is the effective arm the stiffer is the lever. The minimum stiffness depends on the lever's length and the spring's stiffness. In comparison, for the sub-type with movable spring-connection position, the effective arm length of the lever mechanism is R_1 . The longer is the effective arm the stiffer is the lever. The maximum

achievable stiffness therefore depends on the maximum effective arm length and the spring's stiffness coefficient. Therefore, the stiffness range of either the movable force-acting point sub-type or the movable spring-connection position sub-type is related to the length of lever mechanism. The longer is the lever the wider is the range of stiffness regulation. These two sub-types cannot meet the compact and lightweight requirements of force feedback gloves.

In contrary, the maximal and minimal stiffness of the movable pivot sub-type depend on the ratio of R_1 to R_2 , which are independent of the lever's length and the spring's stiffness. Therefore, we choose the movable pivot sub-type in our design solution.

As shown in Fig. 1-a), in the movable pivot sub-type, the acting point of the external force and the spring connection position are fixed, and the pivoting position of the lever changes. According to the principle in [20], when the rotation angle of the lever and the stiffness of the spring are constant, the output stiffness of the mechanism can be tuned by changing the pivoting position of lever. The stiffness can be derived as the following equation:

$$k = \partial T / \partial \beta = 2k_s (R_1 / R_2)^2 (R_1 + R_2)^2 \cos \beta \quad (1)$$

where k and k_s denote the output stiffness of the lever mechanism and the stiffness of the spring, respectively; F is the external force applied to the lever; T and β are the equivalent torque and the deflection angle under the external force F , respectively.

B. Design of Variable Stiffness Unit

For existing variable stiffness mechanism with a movable pivot, the adjustment methods of the pivoting position include rack and pinion mechanism [21], screw slider mechanism [20] and planetary gear mechanism [17]. Since both screw slider mechanism and planetary gear mechanism require a large assembly space and their dead weights are relatively large, the rack and pinion transmission mechanism is adopted in our design.

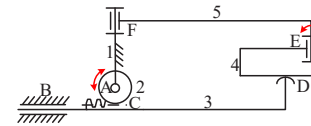


Figure 2. Kinematics diagram of the variable stiffness mechanism

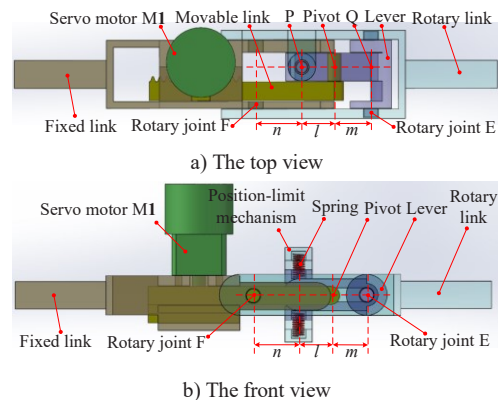


Figure 3. The virtual prototype of the variable stiffness mechanism in SolidWorks

In the mechanical realization of variable stiffness unit, as shown in Fig. 2 and Fig. 3, a servo motor M_1 is rigidly attached to the fixed link (link 1) and drives the movable link (link 3) through a gear (link 2). The other end of the movable link is the pivot, which is connected to the lever (link 4). When only servo motor M_1 runs, the pivoting position is changed with the movement of the movable link. The movable link, the fixed link and the gear form three kinematic pairs (a revolute pair A; a prismatic pair B; a higher gear pair C). Two symmetrically arranged springs are connected on one side to the lever and on the other side to the rotary link (link 5). When the pivot is at a certain position and the rotary link rotates, the movable link, the fixed link, the lever and the rotary link form a higher pair D and two revolute pairs E, F.

The rotation angle of the rotary link is constrained in the range of ± 15 degrees by the limiting mechanism of the variable stiffness unit. When the rotation angle is the maximum value, the deformation of spring reaches up to the maximum value.

Due to the difference of the rotation center between the rotary link and the lever as shown in Fig. 4, when the rotation angle of the rotary link is α , the lever rotates from the initial position (green line) to a certain angle (blue line) and its rotation angle is β . The angle deflection between the lever and the rotary link can be found as:

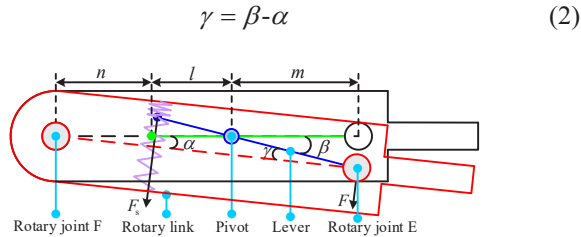


Figure 4. The schematic of stiffness adjustment principle

It is assumed that the springs only deform along the axial direction during the deformation process, and there is no radial shear deformation. Therefore, the force F_s generated by the springs would be:

$$x = (l + m) \sin \gamma \quad (3)$$

$$F_s = k_s (\Delta + x) - k_s (\Delta - x) = 2k_s x \quad (4)$$

where x and k_s denote the deformation distance and the stiffness coefficient of the spring, respectively; l and m denote the distance from the pivot to point P and point Q, respectively; Δ is the pre-deformation of the spring, which is the half of the total deformation.

Since the lever is connected from the other side to the rotary link, therefore the force F applied to the lever by the rotary link can be derived as:

$$F = F_s l / m \quad (5)$$

Because the springs connect the lever and the rotary link, F_s acts on both the rotary link and the lever. Under the action of the force F_s and the force F' , the resultant torque applied to the rotary link can be written as:

$$T = F_s n + F' (l + m + n) \quad (6)$$

where n denotes the distance between the center of rotary joint F and point P. The force F' is the reaction force of the force F . According to the geometric relationship, the relationship between γ and α can be obtained as:

$$m \sin \gamma \approx (l + n) \sin \alpha \quad (7)$$

Thus, the stiffness of the mechanism can be formulated as follow:

$$K = \partial T / \partial \alpha = 2k_s \cos \alpha (m + l)^2 (n + l)^2 / m^2 \quad (8)$$

At equilibrium position, the stiffness can be written as:

$$K = \partial T / \partial \alpha = 2k_s (m + l)^2 (n + l)^2 / m^2 \quad (9)$$

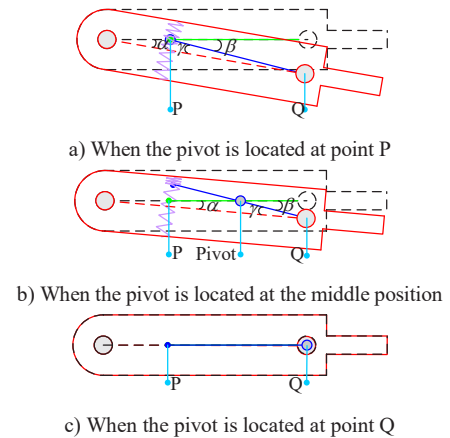


Figure 5. The stiffness varying process

Fig. 5 shows the varying process of stiffness when the pivot is located at point P, the middle position and point Q, respectively. As the pivot moves from point P to point Q, m decreases and l increases. According to (9), stiffness K also increases. The acting point of force coincides with the position of pivot when the pivot moves to point Q, the theoretical stiffness is infinity and angle α approaches to 0 degree. Therefore, the stiffness of the variable stiffness unit can be tuned by changing the position of the pivot along the lever.

III. DESIGN OF THE SINGER-FINGER FORCE FEEDBACK GLOVE

A. Physical Prototype

As shown in Fig. 6 and Fig. 7, the variable stiffness unit (link 12) is fixed on the back of user's hand (link 6) by the velcro. The intermediate link (link 11) connects with the variable stiffness unit and the distal link (link 10) through revolute pairs (K and L). The other end of distal link transmits feedback force to fingertip through the finger cap. The device is made of resin material by 3D printing and the total weight of the mechanism is 55g.

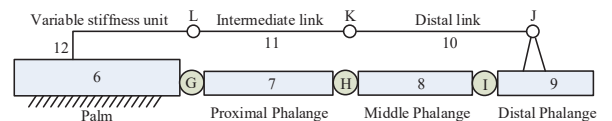


Figure 6. Kinematics diagram of the force feedback glove

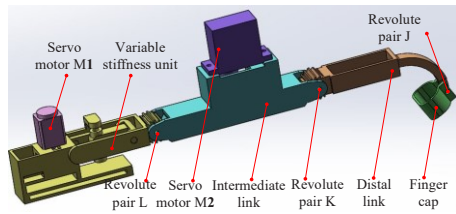
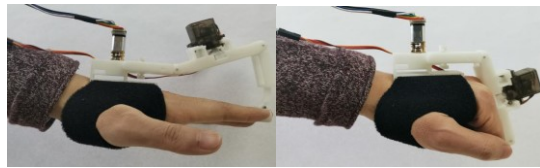


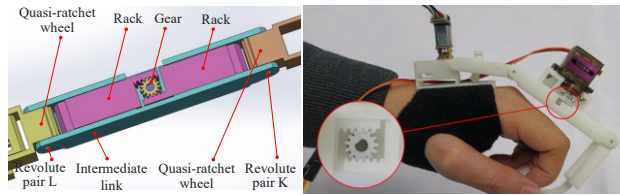
Figure 7. The force feedback glove in SolidWorks

In simulating free space, the pivot of the variable stiffness unit is located at point Q. The revolute pair K and L are working in the unlocked state, i.e. the two pairs rotate as user's finger bends. As shown in Fig. 8, the motion range of the finger is large enough to achieve full extension and full flexion, which can simulate diverse grasping postures. The maximum backdrive force is measured to be 0.069N, which is caused by the friction force at each kinematic pair, the gravity force and inertial force of each link.



a) At the full extension state b) At the full flexion state

Figure 8. The motion state of the glove in simulating free space



a) The glove locking mechanism b) The half-closure grasping posture

Figure 9. The motion state of the glove in simulating constrained space

The conversion process of the free space state and the constrained space state is illustrated in Fig. 9-a). While simulating constrained space, the servo motor M_2 drives two racks by the gear, and locks the quasi-ratchet wheel firmly in place. At the same time, the variable stiffness unit is activated and the stiffness is tuned by the way that servo motor M_1 drives the movable link to change the position of pivot.

As shown in Fig. 9-b), the pivot is located at the middle position and the two revolute pairs are in the locked state. When user's finger bends, the finger cap provide the feedback force that is perpendicular to the fingertip.

B. Control System

The control system includes PC, Arduino UNO R3, servo motor M_1 and M_2 . Arduino UNO R3 communicates with PC through the serial port and controls the rotation of the two servo motors. The parameters of servo motor M_1 are as follows: the rated speed is 1000 r/min, the rated voltage is 12v, the rated torque is 9.8mNm and the mass is 11g. Servo motor M_1 can achieve the position control of pivot using Increment Hall Encode and its theoretical accuracy is 0.081mm. For the servo motor M_2 , its rated voltage is 5v and the rated speed is 83.3 r/min, and the weight is 13g. It is important that the two servo motors are only used for

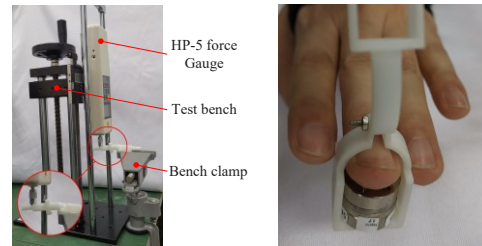
regulating structural stiffness and the conversion process, and the power consumption of the glove is not increased along with the increase of the simulated stiffness of virtual object.

The response time of the glove greatly depends on the type of the implemented actuator. The distance between point P and point Q is 15mm. Under the rated speed of servo motor M_1 , the theoretical movement time is 41ms when the pivot moves from point P to point Q, but the actual movement time is 75ms measured by Increment Hall Encode. For the conversion process, the required rotation angle of servo motor M_2 is 35 degrees and its working time is 70ms. This actual response time is greater than the delay a human can perceive between visual and haptic stimuli (45ms) [13], and the actuation time delay could be further reduced by substituting servo motor M_1 and M_2 by other type of motors with a higher velocity.

IV. PERFORMANCE ANALYSIS

A. Performance of Variable Stiffness

In order to evaluate the characteristics of the variable stiffness unit, the output stiffness of the unit was measured when the pivot locates at point P, the middle position and point Q, respectively. The fixed link was fixed on the bench clamp as illustrated in Fig.10-a), HP-5 force Gauge (HANDPI, China) was fixed on the test bench and drove the rotary link to rotate.



a) Stiffness performance test b) Installation method of the sensor

Figure 10. Test equipment of the glove performances

The corresponding stiffness is 136.96Nmm/rad, 1333.71Nmm/rad and 3368.99Nmm/rad, when rotation angle of rotary link is 10, 5 and 3 degrees and the pivot is located at point P, the middle position and point Q, respectively. Experimental results show that the output stiffness increases with the distance between point P and pivot. When the pivot is located at point Q, the theoretical stiffness is infinity and the rotation angle of rotary link is 0 degree. However, due to the influence of machining error and material's elasticity modulus, the device would produce a small deformation and the maximum stiffness cannot reach to infinity.

B. Performance of Free Space Simulation

Back-drivability is the important index to quantify the performance of a force feedback glove. For a high-fidelity force feedback glove, the resistance force should be as small as possible to avoid obstructing the movement of finger when simulating free space. Using the measurement system [22], we measured the resistance force during the free motion of the fingers. The pivot was located at point Q and revolute pair K and L were in unlocked state. The user moved the finger at a nearly constant velocity back and forth. In the experiment, ATI Nano17 force sensor was used for data collection and its installation method was shown in Fig. 10-b).

As showed in Fig. 11, the maximum resistance force is 0.069N in simulating free space.

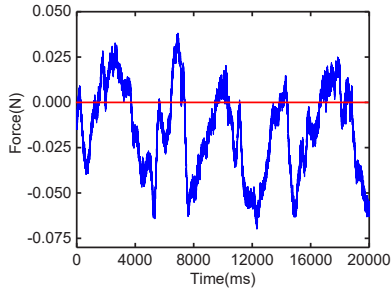


Figure 11. Normal force signal during the free space simulation

C. Performance of Constrained Space Simulation

Force feedback glove should not only simulate the sensation of free space, but also need to provide enough feedback force to simulate the sensation of constrained space. According to the research in Section II B, when the pivot is located at point Q and revolute pair K and L are in the locked state, the force feedback glove forms a rigid body and its feedback force reaches up to the maximum value. And the feedback force on fingertip can be obtained as:

$$F_f = K\alpha/X_f \quad (10)$$

where X_f denotes the distance between the center of rotary joint F and the fingertip.

TABLE I. SAMPLING POINTS ALONG THE TRAJECTORY OF MIDDLE FINGER

Sampling Point	Metacarpophalangeal (degree)	Proximal Interphalangeal (degree)	Distal Interphalangeal (degree)
P ₁	0	0	0
P ₂	20	30	0
P ₃	40	75	30
P ₄	80	90	50

In this experiment, four sampling points of middle finger were selected to evaluate the performance of feedback force as detailed in Fig. 12 and Table I. In each case of the sampling point, the maximum feedback force was measured, respectively.

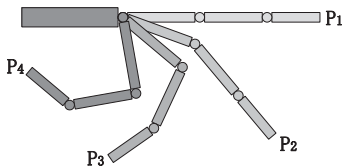


Figure 12. Sampling points along the trajectory of middle finger

As illustrated in Fig. 13, the maximum feedback force at all sampling points is greater than 11N (as shown by the dotted line), and the maximum value is 12.76N at P₃. The ascent and descent of the curves in the figure represent the process of closing and opening of the hand, respectively. The slope of the curves is caused by the difference between the opening and closing speeds of the hand. Due to the limitation of the material property, the exoskeleton would produce a small deformation with the increase of feedback force. In the later improvement scheme, the device would be manufactured with a light but stiffer material.

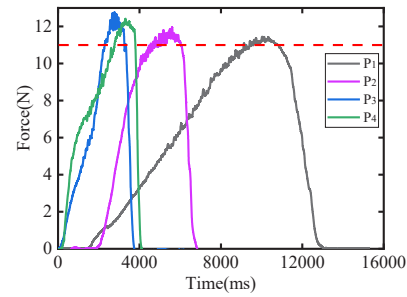


Figure 13. Normal force signal under different sampling points

V. DISCUSSION

Table II provides details for comparison with our single-finger force feedback glove and other devices. Compared with previous force feedback gloves using electric motors and transmission cables [10, 11], the proposed solution has the advantages of lightweight and low power consumption, and can ensure the safety of the users' finger because of its passive structure. Compared with previous force feedback gloves using brakes [12, 13], our solution can simulate variable stiffness while preserving the light weighted structure.

TABLE II. COMPARISONS WITH OTHER FORCE FEEDBACK GLOVES

Glove Name	Our glove	CyberGrasp	RML glove	Dexmo	Wolverine
Stiffness type	Variable	Variable	Variable	Constant	Constant
Actuator type	Servo motor	DC motor with cable driven	DC motor	Micro servo unit	DC motor
Maximum fingertip force (N)	12.76	12	10	—	106
Minimum resistance force (N)	0.069	—	0.2	—	—
Response time (ms)	75	—	30	20-40	21
Per finger weight (g)	55	90	90	54	13.75

However, rigorous work needs to be performed to improve the performance of the proposed force feedback glove. First of all, compared with existing gloves driven by electric motors (shown in Table II), our glove has a longer response time because servo motor M₁ and M₂ have the relatively low rated speed, which results in the response time greater than 45ms. In the future, we will adopt a servo motor with a higher rated speed to reduce the response time. For example, the theoretical response time of Maxon EC8 468334 is 27.28ms and the total weight of servo motor and motor gearbox is 9.2g. The actual response time of the new motor is expected to be reduced down to less than 45ms, which satisfies the requirement a human can perceive between visual and haptic stimuli.

Second, the theoretical maximum stiffness of variable stiffness unit is infinity, but the actual maximum stiffness is 3368.99Nmm/rad in the experiment. In addition, the maximum stiffness of glove is related with the elasticity modulus of material, we will look for a new material with greater elasticity modulus for next generation prototypes. In

order to assess the consistency of the device's stiffness and the perceived stiffness, we will conduct rigorous user studies.

Third, the minimum simulated stiffness of the proposed glove is not zero, and we need to optimize further the structural layout to expand the range of stiffness. Moreover, the glove only has single finger, we will design a new prototype with five fingers to realize the cooperative operation of five fingers.

VI. CONCLUSION

In this paper, we presented a lightweight variable stiffness mechanism for realizing passive force feedback on fingertip. By modulating the pivot of the lever, the mechanism is able to produce a large range of adjustable stiffness in a fast response, while ensuring small backdrive forces. The stiffness of the glove is tuned by changing its structural stiffness rather than applying torque control at each individual joint of the finger, which ranges from 136.96Nmm/rad to 3368.99Nmm/rad.

A single-finger force feedback glove is built to validate the performance of the proposed mechanism. Experimental results validate that the proposed solution can meet the demand of both the free and constrained space simulations. In simulating free space, the maximum backdrive force is 0.069N. While simulating constrained space, the maximum feedback force is 12.76N. Moreover, the motion range of glove is large enough to achieve full flexion and full extension, which can simulate different grasping postures. In addition, the total weight of the single finger prototype is 55g.

In the next step, we plan to improve the force feedback performance of the proposed mechanism by optimizing its geometrical parameters and by adopting smaller and faster response motors, then we will develop a five-finger force feedback glove based on the mechanism, and perform rigorous user studies to validate the performance of the glove in virtual reality environments.

ACKNOWLEDGMENT

This work is supported by the National Key Research and Development Program under Grant No. 2017YFB1002803, and by the National Natural Science Foundation of China under the grant No. 61572055, and No. 61631010.

REFERENCES

- [1] C. Pacchierotti, S. Sinclair, M. Solazzi, A. Frisoli, V. Hayward, and D. Prattichizzo, "Wearable Haptic Systems for the Fingertip and the Hand: Taxonomy, Review, and Perspectives," *IEEE Transactions on Haptics*, vol. 10, pp. 580-600, Oct.-Dec. 2017.
- [2] D. Wang, M. Song, A. Naqash, Y. Zheng, W. Xu, and Y. Zhang, "Toward Whole-hand Kinesthetic Feedback: A Survey of Force Feedback Gloves," *IEEE Transactions on Haptics*, DOI: 10.1109/TOH.2018.2879812.
- [3] I. Zubrycki and G. Granosik, "Novel haptic glove-based interface using jamming principle," presented at the 10th International Workshop on Robot Motion and Control, Poznan, Poland, July 6-8, 2015, pp. 46-51.
- [4] T. Endo, H. Kawasaki, T. Mouri, Y. Doi, T. Yoshida, Y. Ishigure, H. Shimomura, M. Matsumura, and K. Koketsu, "Five-Fingered Haptic Interface Robot: HIRO III," *IEEE Transactions on Haptics*, vol. 4, pp. 14-27, Jan.-Mar. 2011.
- [5] J. Blake and H. B. Gurocak, "Haptic Glove with MR Brakes for Virtual Reality," *IEEE/ASME Transactions on Mechatronics*, vol. 14, pp. 606-615, Oct. 2009.
- [6] Y. Kuroda, Y. Shigeta, M. Imura, Y. Uranishi, and O. Oshiro, "Haptic Glove Using Compression-Induced Friction Torque," presented at the ASME 2013 Dynamic Systems and Control Conference, Palo Alto, California, October 21-23, 2013, Paper No. DSCC2013-3866.
- [7] R. Zhang, A. Kunz, P. Lochmatter, and G. Kovacs, "Dielectric Elastomer Spring Roll Actuators for a Portable Force Feedback Device," presented at the 14th Symposium on Haptic Interfaces for Virtual Environment and Teleoperator Systems, Alexandria, VA, March 25-26, 2006, pp. 347-353.
- [8] S. Zhongsheng, M. Xiaodong and L. Xiaoning, "Design of a bidirectional force feedback dataglove based on pneumatic artificial muscles," presented at the 2009 International Conference on Mechatronics and Automation, Changchun, China, August 9-12, 2009, pp. 1767-1771.
- [9] D. J. Cassar and M. A. Saliba, "A force feedback glove based on Magnetorheological Fluid: Preliminary design issues," presented at the 15th IEEE Mediterranean Electrotechnical Conference, Valletta, Malta, April 26-28, 2010, pp. 618-623.
- [10] CyberGlove Systems. (2013) Cybergrasp. [Online]. Available: <http://www.cyberglovesystems.com/>
- [11] Z. MA and P. Ben-Tzvi, "RML Glove-an Exoskeleton Glove Mechanism With Haptics Feedback," *IEEE/ASME Transactions on Mechatronics*, vol. 20, pp. 641-652, Apr. 2015.
- [12] X. Gu, Y. Zhang, W. Sun, Y. Bian, D. Zhou, and P. O. Kristensson, "Dexmo: An Inexpensive and Lightweight Mechanical Exoskeleton for Motion Capture and Force Feedback in VR," in *Proceedings of the 2016 CHI Conference on Human Factors in Computing Systems*, San Jose, 2016, pp. 1991-1995.
- [13] I. Choi, E. W. Hawkes, D. L. Christensen, C. J. Ploch, and S. Follmer, "Wolverine: A wearable haptic interface for grasping in virtual reality," presented at the 2016 IEEE/RSJ International Conference on Intelligent Robots and Systems, Daejeon, South Korea, October 9-14, 2016, pp. 986-993.
- [14] Y. Wang and L. Fang, "Principle and Design of Mechanically Musculoskeletal Variable-Stiffness Mechanism," *Robot*, vol. 4, pp. 506-512, Apr. 2015.(in Chinese)
- [15] R. Van Ham, B. Vanderborght, M. Van Damme, B. Verrelst, and D. Lefeber, "MACCEPA, the mechanically adjustable compliance and controllable equilibrium position actuator: Design and implementation in a biped robot," *Robotics and Autonomous Systems*, vol. 55, pp. 761-768, Oct. 2007.
- [16] T. Huang, H. Huang and J. Kuan, "Mechanism and Control of Continuous-State Coupled Elastic Actuation," *Journal of Intelligent & Robotic Systems*, vol. 74, pp. 571-587, Jun. 2014.
- [17] S. S. Groothuis, G. Rusticelli, A. Zucchelli, S. Stramigioli, and R. Carloni, "The Variable Stiffness Actuator vsaUT-II: Mechanical Design, Modeling, and Identification," *IEEE/ASME Transactions on Mechatronics*, vol. 19, pp. 589-597, Apr. 2014.
- [18] B. Vanderborght, N. G. Tsagarakis, R. Van Ham, I. Thorson, and D. G. Caldwell, "MACCEPA 2.0: compliant actuator used for energy efficient hopping robot Chobino1D," *Autonomous Robots*, vol. 31, p. 55, Jul. 2011.
- [19] O. Masahiko, I. Nobuyuki, N. Yuto, and I. Masayuki, "Stiffness readout in musculo-skeletal humanoid robot by using rotary potentiometer," presented at the SENSORS, 2010 IEEE, Kona, USA, November 1-4, 2010, pp. 2329-2333.
- [20] A. Jafari, N. G. Tsagarakis and D. G. Caldwell, "AwAS-II: A new Actuator with Adjustable Stiffness based on the novel principle of adaptable pivot point and variable lever ratio," presented at the 2011 IEEE International Conference on Robotics and Automation, Shanghai, China, May 9-13, 2011, pp. 4638-4643.
- [21] N. G. Tsagarakis, I. Sardellitti and D. G. Caldwell, "A new variable stiffness actuator (CompAct-VSA): Design and modelling," presented at the 2011 IEEE/RSJ International Conference on Intelligent Robots and Systems, San Francisco, CA, September 25-30, 2011, pp. 378-383.
- [22] Y. Zheng, D. Wang, Z. Wang, Y. Zhang, Y. Zhang, and W. Xu, "Design of a Lightweight Force-Feedback Glove with a Large Workspace," *Engineering*, vol. 4, pp. 869-880, Dec. 2018.